Tuning Fe Nucleation Density with Charge Doping of Graphene Substrate

Wenmei Ming[1] and Feng Liu[1,*]

[1]*Department of Materials Science and Engineering, University of Utah, Salt Lake City, UT 84112*

(Dated: June 3, 2014)

We have demonstrated that the island nucleation in the initial stage of epitaxial thin film growth can be tuned by substrate surface charge doping. This charge effect was investigated using spin density functional theory calculation in Fe-deposition on graphene substrate as an example. It was found that hole-doping can apparently increase both Fe-adatom diffusion barrier and Fe inter-adatom repulsion energy occurring at intermediate separation, whereas electron-doping can decrease Fe-adatom diffusion barrier but only slightly modify inter-adatom repulsion energy. Further kinetic Monte Carlo simulation showed that the nucleation island density can be increased up to ten times larger under hole-doping and can be decreased down to ten times smaller than that without doping. Our findings indicates a new route to tailoring the growth morphology of magnetic metal nanostructure for spintronics applications via surface charge doping.

PACS numbers:

arXiv:1406.0490v1 [cond-mat.mtrl-sci] 2 Jun 2014

Because of the ideal two-dimensional honeycomb crystal structure and exotic linear dispersed electronic band structure, graphene has attracted intensive research effort of surface functionalization with external adsorbates in order to incorporate carrier doping [1, 2], magnetism [3, 4], catalysis [5, 6] and superconductivity [7, 8], which are strongly related to the bonding involving orbital hybridization and charge transfer between adsorbate and graphene. Due to its only one-atomic thickness, epitaxial graphene is usually unintentionally doped with finite concentration of free carriers through substrate charge transfer [9]. Wider charge doping can also be realized via electric field effect [10] or substrate doping [11]. The resulting charge effect, on one hand may alter the bonding strength between adsorbate and graphene, affecting Fe adsorption and diffusion [12]; on the other hand, it may modulate the adsorbate-adsorbate interaction [13], affecting adsorbate island nucleation. Similar electronic tailing of adsorbate-substrate and adsorbate-adsorbate interactions were observed experimentally on ultrathin oxide film supported on metallic substrate by varying the thickness of the oxide film [14].

For weakly corrugated metallic surfaces such as M/M(111) (M=Al, Cu, Ag, Au)) [15–18] the perturbation to the adsorbate diffusion barrier due to the existence of surrounding adsorbates beyond the nearest-neighbor distance is comparable to the adsorbate diffusion barrier. The resulting inter-adsorbate repulsion part at intermediate distance leads to effective increase of diffusion barrier, giving rise to the significantly larger nucleation island density observed than from mean-field nucleation theory, which includes only nearest-neighbor interaction. Recent experiment of Fe deposited on epitaxial graphene on 6H-SiC(0001) [19] reported that island density increased almost linearly with depositon amount up to 2.5 ML without appearance of saturation and showed weak temperature dependence. These are the indications of graphene being another weakly corrugated system for Fe with sizeable inter-adatom repulsion at distance larger than nearest-neighbor distance. Further DFT calculation predicts the electronic origin of the Fe-Fe repulsion [20].

In this work we are motivated to study the charge doping effects on the Fe adsorption, diffusion and adatom-adatom interaction on graphene substrate. We found that hole-doping increases the adsorption energy, diffusion barrier and Fe-Fe repulsion energy, and that electron-doping decreases the diffusion barrier but only modifies slightly the adsorption energy and Fe-Fe repulsion energy. It is therefore expected that higher Fe island density can be achieved by hole doping and more layer-like film can be achieved by electron doping. Further kinetic Monte Carlo (kMC) simulations shows that Fe nucleation island density can be tuned from being six times larger under hole doping to being ten times smaller under electron doping than the zero-doping case. This wide-range tunability may provide the potential to grow Fe film with island morphology as magnetic storage device and more uniform layer morphology as magnetic electric contact for spin injection in spintronic applications.

The spin density functional theory (DFT) calculations were performed by using projector augment wave pseudopotential (PAW) [21] with the generalized gradient approximation (GGA) [22] to the exchange-correlation functional, as implemented in VASP package [23]. 7×7 graphene supercell plus 13 Å vacuum was used as the substrate. 400 eV energy cutoff and $3 \times 3 \times 1$ Γ-centered k-mesh were used for wavefuntion expansion and k-space integration, respectively. Charge doping was simulated by adding (removing) electron for electron (hole) doping and compensating opposite charge background to keep the system neutral. The charge was varied from hole concentration of $-1.17 \times 10^{14}\ e/cm^2$ to electron concentration of $0.78 \times 10^{14}\ e/cm^2$. One Fe adatom was used to calculate the adsorption energy, diffusion barrier and magnetic property. Two Fe atoms with varying separation were used to calculate the inter-atom interaction energy.

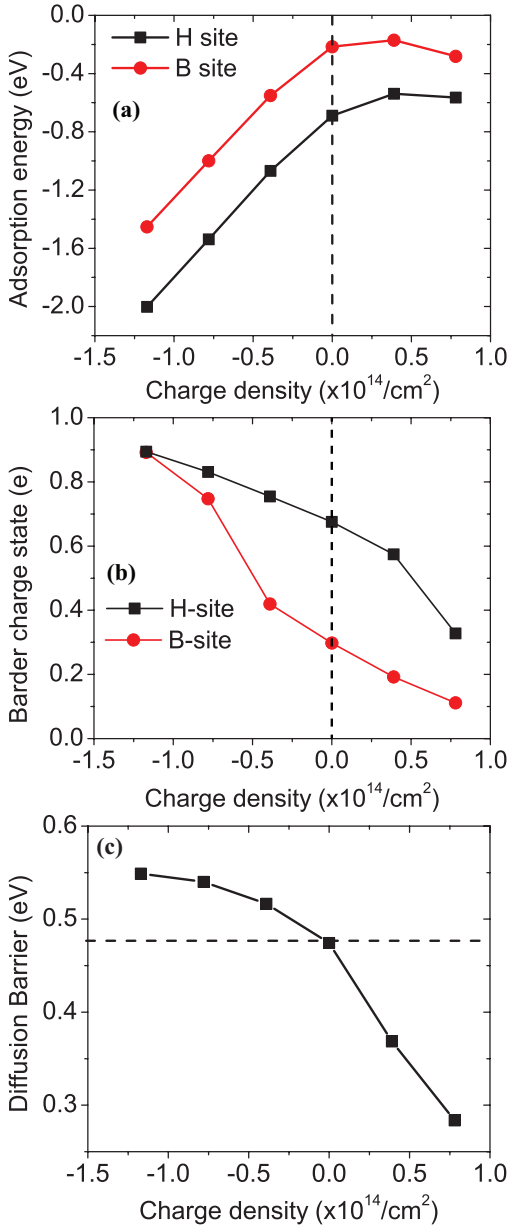

FIG. 1: (color online) (a) Adsorption energy versus charge doping concentration for Fe adatom at H-site and B-site; (b) Bader charge of Fe adatom at H-site and B-site versus charge doping concentration; (c) diffusion barrier versus charge doping concentration.

All the structures were relaxed in terms of internal atomic coordinates using conjugate gradient method until the force exerted on each atom is smaller than 0.01 eV/$\mathring{A}^3$. The transition saddle point along adatom diffusion path was identified using nudged elastic band method [24].

First we found that within the doping concentration considered here Fe adsorption site is the hollow site (H-site) and the transition saddle point is the bridge site (B-site). The adsorption energy E_{ad} is defined as $E_{ad} = E(Graphene+Fe) - E(Graphene) - E(Fe)$, where $E(Graphene + Fe)$ is the energy of adatom+graphene, E(Graphene) is the energy of clean graphene with charge doping and E(Fe) is the energy of isolated Fe atom. It is plotted as a function of charge doping concentration for both Fe at H-site and Fe at B-site in Fig. 1(a). With respect to zero-charge doping case hole doping increases rapidly the adsorption energy but electron doping only slightly changes the adsorption energy. During the process of Fe adsorption on graphene, it has graphene π bond breaking and Fe-C bond formation, so the adsorption energy will be proportional to the bond energy difference between Fe-C and graphene π. The charge doping dependence of Fe-C bond energy and graphene π bond energy will give rise to the trend of Fe-adsorption energy variation as a function of charge doping concentration. For graphene π bond it will have lower bond energy because less bonding states will be occupied under hole doping, and also lower bond energy because more antibonding states will be occupied under electron doping. For Fe-C bond, it involves charge transfer and orbital hybridization. The energy gain due to the charge transfer is proportional to the difference between electron energy levels of Fe atom before adsorption and the Fermi energy of graphene. For clean graphene electron doping decreases its Fermi energy and hole doping increases its Fermi energy, so the difference between electron energy levels of isolated Fe atom and substrate Fermi energy will become larger for hole doping indicating charge transfer from Fe to grapene will be easier, but smaller for electron doping indicating charge transfer from Fe to graphene will be blocked. Therefore the combined effect of graphene *pi* bond breaking and charge transfer may increase Fe adatom adsorption energy with hole doping but only slightly varies with electron doping.

We further calculated the change of Fe adatom charge transfer in response to graphene work function change (equivalently Fermi energy change) under charge doping in Fig. 1(b). The amount of charge transfer from Fe adatom to graphene is represented by Bader charge. As argued above, there are more charge transfer under hole doping and less charge transfer for both Fe at H-site and B-site. We may estimate the adsorption energy gain from charge transfer part using the following model:

$$E_{ad}(q) = E_r(q) - q\phi \tag{1}$$

where q is the adatom charge transfer, ϕ is the graphene substrate work function and E_r is remaining contribution to the adsorption energy. The E_{ad} variation due to the change of ϕ can be estimated with respect to ϕ of no-doping graphene using:

$$\Delta E_{ad}(q) = \Delta E_r(q) - q\Delta\phi - \phi\Delta q \tag{2}$$

Three contributions are include in the variation of E_{ad}. While it is not clear to see in what fashion the first one $\Delta E_r(q)$ changes E_{ad}, we can easily see that the second

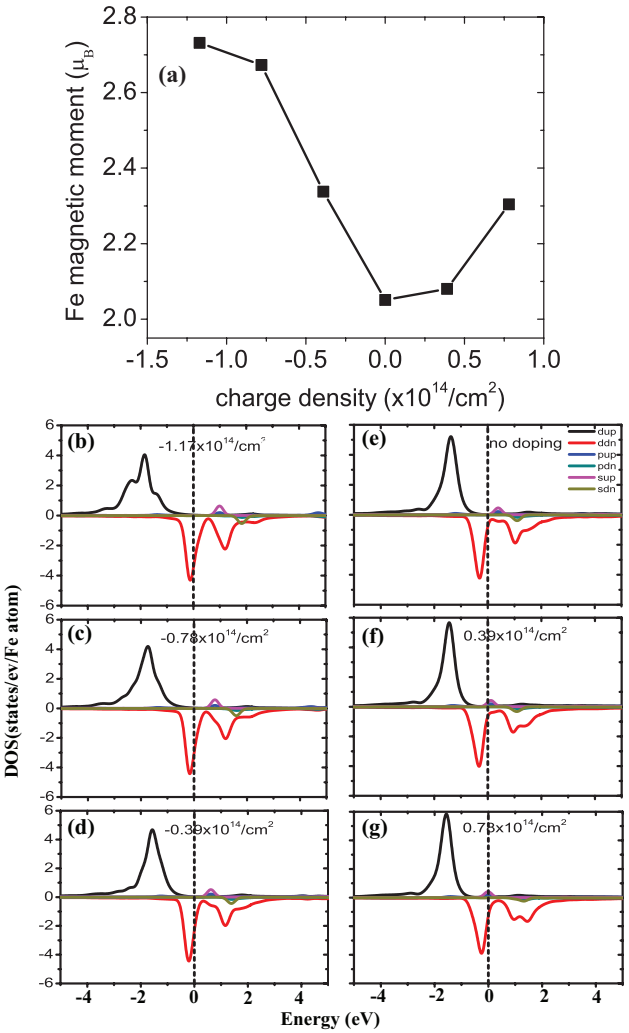

FIG. 2: (color online) (a) Local magnetic moment of Fe adatom of H-site versus charge doping concentration; (b-g) Fe adatom partial density of states with projection to s, p, d orbitals for both spin-up and spin-down components.

term increases E_{ad} in hole doping when the work function increases but decreases E_{ad} in electron doping when the work function decreases. Similarly the third term increases E_{ad} in hole doping when the charge transfer q is increased but decreases E_{ad} in electron doping when the charge transfer q is decreased.

The Fe-adatom diffusion barrier is shown in In Fig. 1(c) as a function of charge doping concentration. Without charge doping, the diffusion barrier is 0.48 eV [25], in good agreement with previous report. With hole doping the diffusion barrier can be increased to 0.55 eV but with electron doping diffusion barrier can be decreased to 0.28 eV. This trend can be again understood from the charge doping effect on the adsorption energy of Fe at H-site and B-site. The diffusion barrier is the adsorption energy difference between Fe at B-site and Fe at H-site, we thus express diffusion barrier E$_d$:

$$E_d(q) = E_r^B(q) - E_r^H(q) - (q_B - q_H)\phi \qquad (3)$$

The first order variation of E_d in charge doping will then be:

$$\begin{aligned}\Delta E_d(q) =& \Delta(E_r^B(q) - E_r^H(q)) - (q_B - q_H)\Delta\phi \\ & - (\Delta q_B - \Delta q_H)\phi\end{aligned} \qquad (4)$$

The second term indicates that a direct tuning of work function ϕ will lead to a variation of diffusion barrier depending on the sign of work function change and the magnitude. Because work function is increased with hole doping, this term gives rise to an increase of diffusion barrier. On the other hand, because work function is decreased with electron doping, this term gives rise to an decrease of diffusion barrier. This predication is consist with the trend of diffusion barrier in Fig. 1(c) calculated from DFT. We thus believe the work function tuning should be the dominant role in varying the Fe-adatom diffusion barrier.

For no-charge doping graphene+Fe adatom, previous work [26, 27] has shown that because of the hybridization between Fe 3d states and graphene p states, the Fe 4s states are shifted to higher energy relative to Fe 3d states upon adsorption and originally two occupying two 4s electrons are transferred mainly to Fe 3d states, resulting in the Fe local magnetic moment reduction from 4 μ_B to about 2 μ_B. Such a situation is expected to be further modified upon charge doping, which may change the Fe adatom orbital occupation. In Fig. 3(a) we show the Fe adatom local magnetic moment versus the charge doping concentration. Hole doping significantly increases the magnetic moment from 2.05 μ_B to 2.73 μ_B, and electron doping modestly increases the magnetic moment to 2.32 μ_B. In Fig. 3(b) the density of states under different charge doping concentration are plotted, from which we can see the different Fe adatom orbital occupation which leads to the Fe magnetic moment variation with charge doping. Starting from zero-doping to increasing hole doping, the occupation of spin-down component of Fe d-orbital keeps decreasing and the occupation of spin-up component is unchanged. This leads to the further imbalance between spin-up and spin-down states and leads to increased Fe magnetic moment. With increasing electron doping, the slight decrease in Fe spin-down d-orbital occupation and increase in Fe spin-up s-orbital result in the slow increase of Fe magnetic moment.

Next we calculated Fe adatom-adatom interaction energy as a function of the separation under different charge doping. Six configurations are considered as shown in Fig. 4(a). For clarity we separated nearest-neighbor (NN) adatom-adatom interaction (configuration 1) which represents the direct chemical bonding from the beyond NN adatom-adatom interaction. They are shown in Fig.

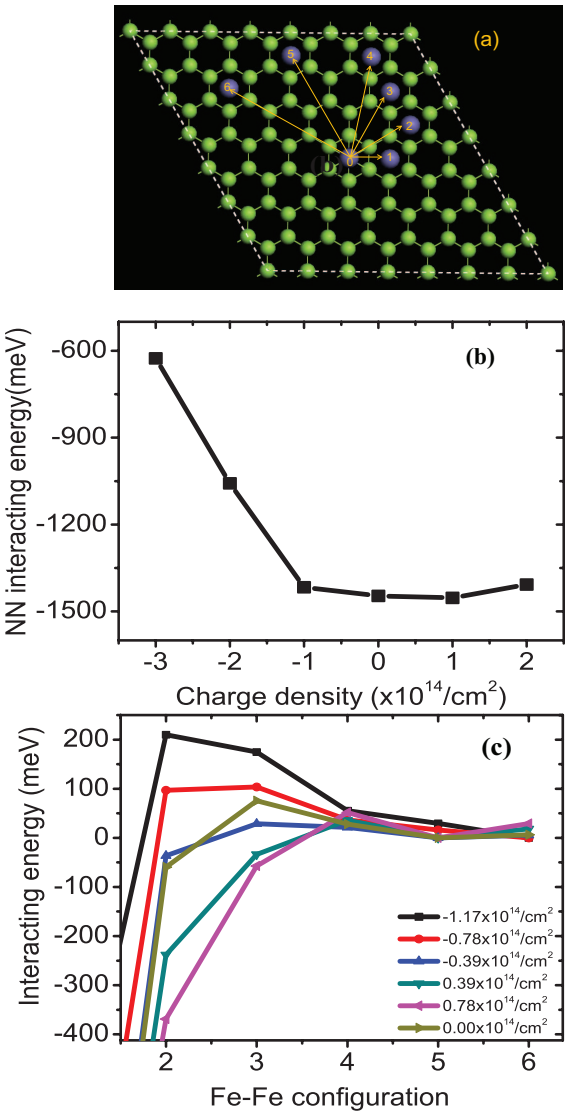

FIG. 3: (color online) (a) Interaction energy between two nearest-neighboring Fe adatoms; (b) Interaction energy as a function of separation beyond nearest-neighbor.

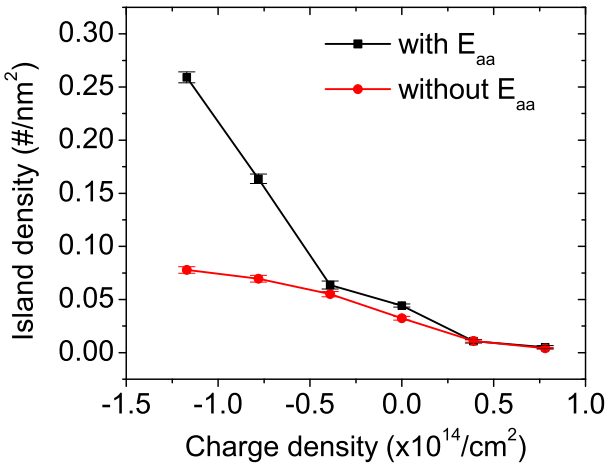

FIG. 4: (color online) KMC simulated island density as a function of charge doping concentration for both cases of with adatom-adatom interaction (with E_{ad}) and without adatom-adatom interaction (without E_{ad}).

4(b) and Fig. 4(c), respectively. The NN interaction energy is only changed very little under the charge doping concentration from $-0.39\times10^{14}/cm^2$ to $0.78\times10^{14}/cm^2$. However, one observes that further hole doping decreases the NN interaction energy rapidly and the the NN interaction energy is reduced a lot to 0.60 eV under hole doping of $-1.17\times10^{14}/cm^2$ with respect to 1.45 eV for no-doping situation. Recalling the Bader charge in Fig. 1(b), because the Bader charge keeps decreasing from hole doping to electron doping, we may attribute this reduction of NN interaction energy to the significantly increased repulsive Coulomb interaction under large hole doping and only a lot weaker dipole-dipole repulsive interaction under the doping concentration from $-0.39\times10^{14}/cm^2$ to $0.78\times10^{14}/cm^2$. In Fig. 4(c) within the doping concentration considered in the work, the adatom-adatom distance at which they display repulsive interaction persistly exists. Apparently, the repulsive peak is pushed gradually towards to be at next NN distance and increased from electron doping to hole doping.

The charge doping effects on the Fe-adatom diffusion barrier and adatom-adatom interaction is expected to be reflected in the Fe nucleation island density of the initial film growth. We next simulated the Fe island density as a function of charge doping concentration using kMC simulation method proposed in Ref.[28]. The simulation cell is $200x200$ graphene supercell. The diffusion barrier and adatom-adatom interactions from DFT calculations above are used as input parameters. The hopping rate with Arrhenius form of $\nu=\nu_0\exp(-E_d/k_BT)$ and position dependent diffusion barrier approximation of $E_d=E_d^0+0.5(E_j-E_i)$ were used. ν_0 is chosen to have constant value of $10^{12}/s$, T is 300 K, E_i and E_j are the interaction energies before and after hopping, respectively. For simplicity irreversible nucleation (no desorption), critical island size of 1 and no edge diffusion are assumed [29, 30]. The deposition rate is 0.01 ML/s and amount of deposition is 0.05 ML. In Fig. 5 we show the island density for both situations with and without including Fe adatom-adatom interaction. From the curve without adatom-adatom interaction, the island density can be decreased to 8 times smaller in electron doping and 3 times larger in hole doping than in zero-doping. Including Fe adatom-adatom interaction, it's most evident for the hole doing larger than -0.39×10^{14}, the island density is significantly increased up to 6 times larger than in zero-doping. For the remaining doping regime, the island density is very close to that without inter-adatom interaction. It indicates that the combined effect of the diffusion barrier and inter-adatom interac-

tion on the island density only takes place in large hole doping and the diffusion barrier tuning dominates the change of island density in the rest of the charge doping regime.

To conclude, we have investigated the effect of the charge doping of graphene substrate on Fe nucleation island density, which increases under hole-doping and decreases under electron-doping. The underlying mechanism is from the charge-tuning of Fe-adatom diffusion barrier, which is gradually increased by hole doping but is rapidly decreased by electron doping, and Fe inter-adatom repulsive interaction, which is increased significantly by large hole doping. Additionally Fe local magnetic moment can be tuned significantly with charge doping. The combined effects provide large range of tuning of magnetic island density and tailoring the growth morphology of magnetic metal nanostructure for spintronics applications via surface charge doping.

This work was supported by NSF MRSEC (Grant No. DMR-1121252) and DOE-BES (Grant No. DE-FG02-04ER46148). We thank M. C. Tringides and Y. Han and for fruitful discussions. We acknowledge the CHPC at University of Utah and NERSC for providing the computing resources.

* Corresponding author. E-mail: fliu@eng.utah.edu

[1] Aaron Bostwick *et al*, Nat. Phys. **3**, 36 (2007).
[2] S. Y. Zhou *et al*, Phys. Rev. Lett. **101**, 086402 (2008).
[3] T. Eelbo *et al*, Phys. Rev. Lett. **110**, 136804 (2013).
[4] A. V. Krasheninnikov *et al*, Phys. Rev. Lett. **102**, 126807 (2009).
[5] Shaojun Guo *et al*, Angew. Chem. Int. Ed. **51**, 11770 (2012).
[6] Kun Han *et al*, Appl. Phys. Lett. **104**, 053101 (2014).
[7] S. -L. Yang *et al*, Nat. Commun. **5**, 3493 (2014).
[8] Gianni Profeta *et al*, Nat. Phys. 8, **131** (2012).
[9] C. Riedl *et al*, Phys. Rev. Lett. **103**, 246804 (2009).
[10] Kin Fai Mak *et al*, Phys. Rev. Lett. **112**, 207401 (2014).
[11] Nisha Mammen *et al*, J. Am. Chem. Soc. **133**, 2801 (2011).
[12] J. O. Sofo *et al*, Phys. Rev. B **83**, 081411(R) (2011).
[13] Dmitry Solenov *et al*, Phys. Rev. Lett. **111**, , 115502 (2013).
[14] Livia Giordano *et al*, Phys. Rev. Lett. **101**, 026102 (2008).
[15] Kristen A. Fichthorn *et al*, Phys. Rev. Lett. **84**, 5371 (2000).
[16] Jascha Repp *et al*, Phys. Rev. Lett. **85**, 2981 (2000).
[17] A. Bogicevic *et al*, Phys. Rev. Lett. **85**, 1910 (2000).
[18] Fabien Silly *et al*, Phys. Rev. Lett. **92**, 016101 (2004).
[19] S. M. Binz *et al*, Phys. Rev. Lett. **109**, 026103 (2012).
[20] Xiaojie Liu *et al*, Phys. Rev. B **84**, 235446 (2011).
[21] G. Kresse and D. Joubert, Phys. Rev. B **59**, 1758 (1999).
[22] J. P. Perdew, J. A. Chevary, S. H. Vosko, K. A. Jackson, M. R. Pederson, D. J. Singh and C. Fiolhairs, Phys. Rev. B **46**, 6671 (1992).
[23] G. Kresse and J. Furthmuller, Phys. Rev. B **54**, 11169 (1996).
[24] G. Mills and H. Jonsson, Phys. Rev. Lett. **72**, 1124 (1994).
[25] Oleg V. Yazyev *et al*, Phys. Rev. B **82**, 045407 (2010).
[26] Chao Cao *et al*, Phys. Rev. B **81**, 205424 (2010).
[27] Kevin T. Chan *et al*, Phys. Rev. B **77**, 235430 (2008).
[28] K. A. Fichthorn and W. H. Weinberg, J. Chem. Phys. 95, 1090 (1991).
[29] M. C. Bartelt and J. W. Evans, Phys. Rev. B **46**, 12675 (1992).
[30] H. Brune, Surf. Sci. Rep. **31**, 121 (1998).